Late autumn to spring changes in the inorganic and organic carbon dissolved in the water column at Scholaert Channel, West Antarctica

XIAOMENG WANG[1,2], GUI-PENG YANG[1], DAMIAN LÓPEZ[2], GUSTAVO FERREYRA[2,3], KARINE LEMARCHAND[2] and HUIXIANG XIE[2]*

[1]*Key Laboratory of Marine Chemistry Theory and Technology, Ministry of Education, Ocean University of China, Qingdao, China 266100*
[2]*Institut des sciences de la mer de Rimouski, Université du Québec à Rimouski, Québec, Canada G5L 3A1*
[3]*Instituto Antártico Argentino, Cerrito 1248 (1010) Buenos Aires, Argentina*
huixiang_xie@uqar.qc.ca

Abstract: The temporal changes in dissolved inorganic (DIC) and organic carbon concentrations (DOC) were monitored from late autumn to spring 2006 in the Scholaert Channel, West Antarctic Peninsula. Surface DIC spanned a small range (2163.3 to 2194.5 μmol kg^{-1}), increasing from late autumn to winter and then decreasing in spring. An excess of DOC (7.0–63.6 μmol l^{-1}), against a deepwater background concentration of 44 μmol l^{-1}, existed in the surface mixed layer throughout the sampling period. Mass-balance budgeting indicates that the DIC dynamics were primarily governed by remineralization in winter and by primary production in spring despite very low biomass of both autotrophic and heterotrophic organisms. The net community production (7.3 mmol C m^{-2} d^{-1}) in spring was mainly partitioned to DOC accumulation (3.6 mmol m^{-2} d^{-1}) and downward export of particulate organic carbon (POC) (2.9 mmol m^{-2} d^{-1}) rather than POC accretion (0.8 mmol m^{-2} d^{-1}) in the surface mixed layer. The study area acted as a source of CO_2 to the atmosphere in winter ($\sim$0.8 mmol m^{-2} d^{-1}) and a sink in spring (2.3–5.3 mmol m^{-2} d^{-1}), and hence was not a one-way CO_2 sink as had been previously hypothesized for marginal sea ice zones.

Introduction

The Southern Ocean below 50°S, with 14% of the total ocean surface area, was estimated to be responsible for 24% (0.39 Pg C yr^{-1}) of the global ocean carbon dioxide (CO_2) uptake from the atmosphere (Takahashi *et al*. 2002). However, more recent studies, based on expanded surface seawater CO_2 partial pressure databases, reveal that the oceanic CO_2 sink in the Southern Ocean is much smaller than previously estimated (0.05 Pg C yr^{-1} or 4% of global ocean CO_2 uptake, Takahashi *et al*. 2009) and the potential of the Southern Ocean as a CO_2 sink is decreasing (Metzl 2009, Takahashi *et al*. 2009). This improvement in the CO_2 flux estimate is largely attributed to the new databases capturing more spatiotemporal variations in surface water CO_2, which exhibits a mosaic of saturation state with the presence of both super- and undersaturation relative to atmospheric CO_2 in each season (Takahashi *et al*. 1993, Hoppema *et al*. 1995, 2000, Carrillo & Karl 1999, Gibson & Trull 1999, Stoll *et al*. 1999, Álvarez *et al*. 2002, Carrillo *et al*. 2004, Bertolin & Schloss 2009). However, compared to warmer ocean basins the Southern Ocean is still sparsely sampled and its role in regulating atmospheric CO_2 and in the global ocean carbon cycle remains elusive. Notably,

most of the past CO_2 observations are limited to offshore waters and to summer with few studies conducted in coastal waters, where larger spatial and seasonal changes are expected, and on annual or continuously long-term seasonal scales from which a better evaluation of CO_2 variation can be made (Carrillo & Karl 1999, Gibson & Trull 1999).

Underlying the large spatial, seasonal, and interannual variability of the surface water CO_2 saturation state is the parallel heterogeneity of various physical and biological processes controlling the distribution and evolution of the CO_2 system. In this, the frontal and marginal sea ice zones are especially noteworthy. The frontal zones usually possess a high primary productivity and sequester atmospheric CO_2 by the "biological pump" and through the formation of intermediate water (e.g. in the area of the Antarctic Polar Front), which brings CO_2 from surface water to deeper layers (Fransson *et al*. 2004). In marginal sea ice zones biological activity is synchronized with the ice dynamics with primary production dominating in spring and summer and remineralization prevailing in winter. These areas, therefore, usually act as atmospheric CO_2 sinks in spring and summer and sources in winter (Carrillo *et al*. 2004, Takahashi *et al*. 2009). Amongst the numerous Antarctic marginal sea ice zones, the coastal and shelf areas
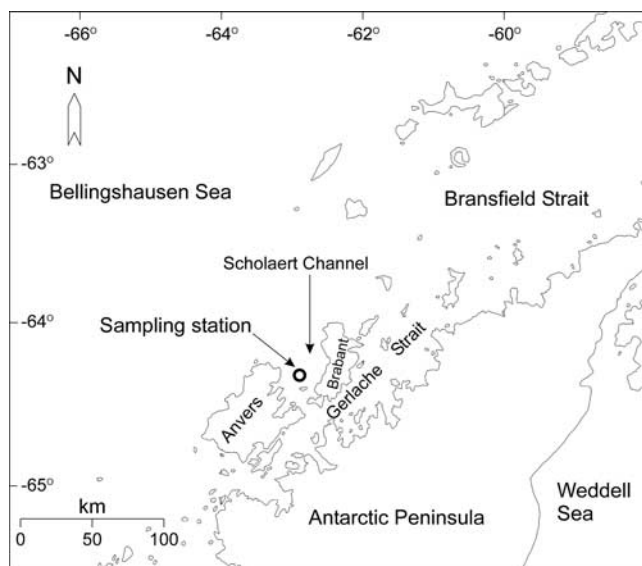
Fig. 1. Map showing sampling station and surrounding areas.

of the West Antarctic Peninsula (WAP) are particularly ideal for testing the effects of climate warming on the marine ecosystem, including the CO_2 system, since the WAP is one of the most rapidly warming regions on Earth (Ducklow *et al*. 2007). Rising temperature has led to later advance and earlier retreat of sea ice, diminishing ice concentration and thickness, and thereby an overall reduced ice extent (Ducklow *et al*. 2007, Stammerjohn *et al*. 2008). This changing ice dynamics has substantially altered and will continue to alter the heat flux between the water column and the atmosphere, the timing and magnitude of the spring phytoplankton bloom, the abundance and composition of organisms at various trophic levels, and the interactions between prey and predators (Ducklow *et al*. 2007). All of these factors are expected to significantly influence the CO_2 system via increased air-sea exchange area, reduced solubility, modified primary production and remineralization, and altered trophic energy transfer and sedimentation.

The cycling of the oceanic CO_2 system closely interacts with that of dissolved organic carbon (DOC), the largest organic carbon pool in the ocean. Primary production, which utilizes dissolved inorganic carbon (DIC), is the main source of DOC while remineralization of DOC is a major contribution to the marine DIC pool. DOC concentrations (DOCs) in the surface ocean usually exceed those in the deep ocean as a result of temporal and spatial uncoupling of *in situ* DOC production (e.g. extracellular release, cell lysis, sloppy feeding, excretion) and loss (e.g. bacterial consumption, photooxidation, downward diffusion) in the upper ocean (Carlson 2002). The dynamics of the excess DOC, therefore, reflects the interactions between various biological and physical processes that control DOC production, loss, and distribution. At present, DOC measurements in Antarctic coastal waters are rare (Ducklow *et al*. 2007) and less is known
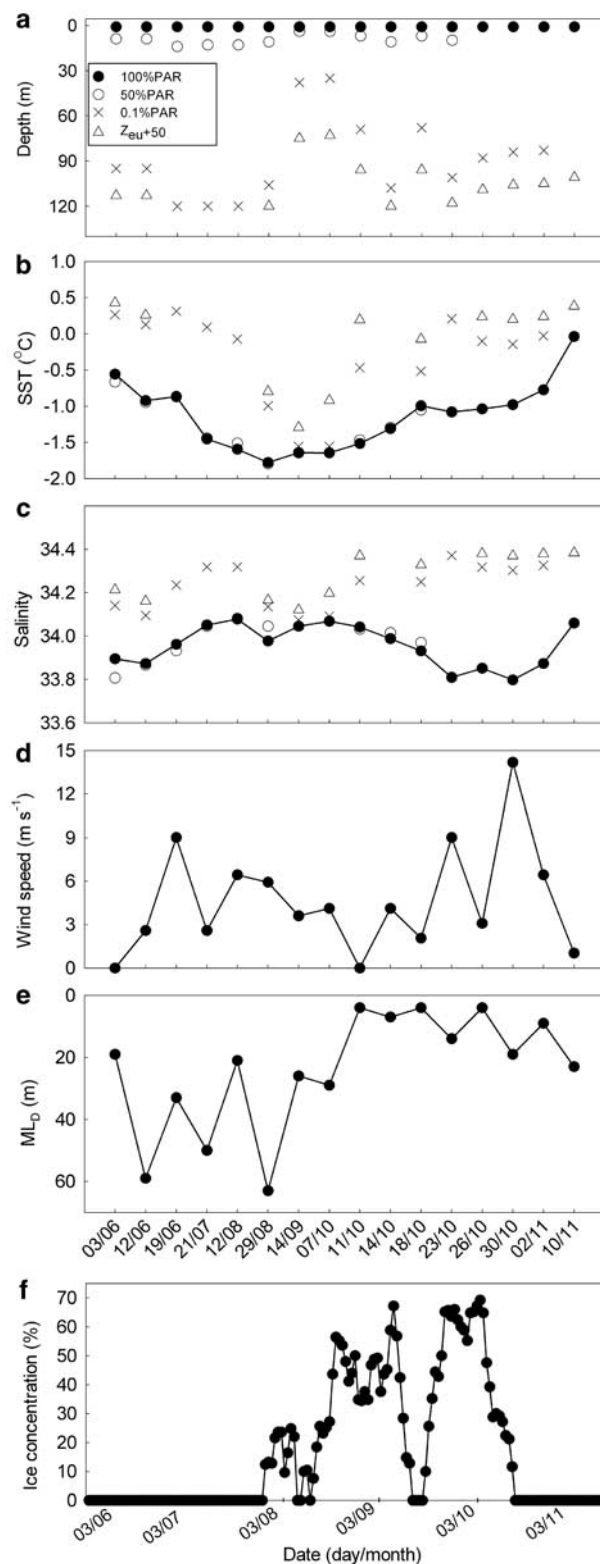

Fig. 2. Temporal variations of **a.** the sampling depth, **b.** seawater temperature, **c.** salinity, **d.** daily averaged wind speed, **e.** surface mixed-layer depth, and **f.** ice concentration. Symbols in panel **b–f** are the same as those in panel **a.** $Z_{eu} + 50$ stands for 50 m below the 1% PAR level.

of its temporal variability than of its spatial heterogeneity (Scott *et al*. 2000). Limited data reveal extraordinary variations in DOC ranging from $> 8333\ \mu mol\,l^{-1}$ during a massive *Phaeocystis* sp. bloom in Prydz Bay (Davidson & Marchant 1992) to more typical values of $52–102\ \mu mol\,l^{-1}$ in the upper mixed layer (ML) in the Bransfield and Gerlache straits (Doval *et al*. 2002) and of $30–258\ \mu mol\,l^{-1}$ at an Antarctic coastal site (68°34'S, 77°57'E) (Scott *et al*. 2000).

This study reports the changes in the CO_2 system and DOC from late autumn to spring at a coastal site off the WAP. CO_2 fluxes between air and sea are estimated and physical and biological processes controlling the CO_2 system are evaluated. Results from this study augment the meagre datasets on DIC and DOC in the coastal areas of the Southern Ocean and help improve the estimates of CO_2 fluxes and the knowledge of DIC and DOC cycling in this climatically sensitive region.

Methods

Sampling

The sampling station (64°19'31"S, 62°53'42"W) was located in the Scholaert Channel flanked by Anvers and Brabant islands off the West Antarctic Peninsula (WAP) (Fig. 1). Water depth at the site is $\sim 150\,m$ and the most important water mass influencing the area originates from the Bellingshausen Sea (García *et al*. 2002). Bulk water was collected with 5 or 12 litre Niskin bottles around 14h00 on each sampling day from 3 June–10 November 2006. During periods of ice cover water was taken from a hole drilled through the ice (7 October only) or from open water near the ice edge (29 August only), $\sim 1\,km$ away from the station. Simultaneous profiling of conductivity, temperature (T), and depth was made with a Seabird CTD (model SBE 19Plus). Sampling depths for DIC and DOC followed those for concurrent biological studies, usually at 100, 50, 0.1% photosynthetically active radiation (PAR) levels with the deepest depth at 50 m below the 1% PAR level (sampling depth vs PAR level is shown in Fig. 2a). Only surface water (100% PAR) was sampled for pH due to logistic and analytical constraints. DIC samples were collected into 120 ml borosilicate glass bottles, sterilized with $25\ \mu l$ saturated mercuric chloride solution, and tightly sealed with Teflon-lined screw caps. The samples were stored in the dark at room temperature and analysed within two weeks of sample collection in a ship based (*Sedna IV*) laboratory in the immediate vicinity of the sampling station. Samples for DOC analysis were passed through $0.2\ \mu m$ Whatman polyethersulphone filters and stored frozen (-20°C) in 60 ml borosilicate glass bottles until analysis. Samples for pH determination were drawn into 60 ml borosilicate glass bottles and analysed upon collection. All glass bottles had been acid-cleaned and thoroughly rinsed with Nanopure water prior to sampling.

DIC and pH bottles were rinsed and then overflowed by around three times their volumes with sample water before the final filling. DOC bottles were pre-rinsed three times with the filtered sample water.

Analysis and calculation

DIC concentrations were measured according to Cai & Wang (1998) using an AS-C2 DIC Analyser (Apollo SciTech Inc, Athens, GA) that comprises a Kloehn versa pump 6 digital dispensing device, a custom made purging vessel, and a LI-COR 6252 CO_2/H_2O analyser. The system was calibrated with the Certified Reference Material (CRM) from A. Dickson (Scripps Institution of Oceanography) at intervals of ~ 2 h or every 10 samples during which deviation of the CRM was $< 0.1\%$. The precision of DIC measurement was $\pm 1\ \mu mol\,kg^{-1}$ based on 10 replicate analyses of the CRM. pH was measured at 25°C with a Ross semi-micro combination pH electrode (Orion Research). Three NBS pH buffers (pH 4.01, 7, 10.01) were used to determine the electrode's response slope and a tris/HCl buffer at salinity 35 to derive a seawater pH scale (Millero *et al*. 1993, Chen *et al*. 2008). The accuracy was ± 0.01 pH units as determined with the CRM. DOC was measured using high temperature catalytic oxidation (HTCO) with a Shimadzu-5000A TOC Analyser. The measurement was standardized with potassium hydrogen phthalate. The precision for 3–5 replicate analyses of each sample was $\sim 1\%$. Chlorophyll *a* (chl *a*) concentrations were measured according to the HPLC method by Zapata *et al*. (2000) with a detection limit of $0.005\ \mu g\,l^{-1}$. A Bran Luebbe AutoAnalyzer 3 system determined the concentration of nitrate and nitrite (nitrate + nitrite) based on the method by Grasshof *et al*. (1983). The precision of the nitrate + nitrite measurement is 0.21%. Free-living heterotrophic bacterial cell abundance was cytometrically determined using an Epics Altra flow cytometer (Beckman Coulter) with a coefficient of variation ranging from 1 to 2% between each measurement. Detailed procedures of chl *a*, nutrients, and bacteria measurements will be published elsewhere (S. Moreau *et al*. unpublished).

The fugacity of CO_2 ($f CO_2$) in seawater was calculated from DIC, pH, temperature, salinity and nutrient data using the CO_2 system programme by Lewis & Wallace (1998) and the apparent thermodynamic dissociation constants of Roy *et al*. (1993, 1994). The accuracy in the $f CO_2$ calculation was estimated to be $< 10\ \mu atm$ based on the errors from pH ($\sim 7\ \mu atm$) and DIC ($\sim 1\ \mu atm$) measurements. CO_2 air-sea flux, FCO_2 ($mmol\,m^{-2}\,d^{-1}$), was computed using the following equation:

$$FCO_2 = 0.24\,K_0\,k\,\Delta f CO_2 \qquad (1)$$

where k is the piston velocity of CO_2 ($cm\,h^{-1}$), the factor 0.24 converts k from $cm\,h^{-1}$ to $m\,d^{-1}$, K_0 is the solubility of CO_2 ($mmol\,m^{-3}\,atm^{-1}$) calculated according to Weiss (1974), and $\Delta f CO_2$ the difference in CO_2 fugacity (μatm)

between seawater and atmosphere. The piston velocity was calculated according to the formula of Liss & Merlivat (1986), which expresses k as a function of wind speed and the CO_2 Schmidt number, the latter being obtained from Wanninkhof (1992). The mean error in FCO_2 over the whole sampling period was estimated to be ± 1.3 mmol m^{-2} d^{-1} or $\pm 55\%$ using the errors of $1\,m\,s^{-1}$ in wind speed, $10\,\mu$atm in seawater fCO_2, and $0.1\,\mu$atm in atmospheric fCO_2. We chose the Liss & Merlivat (1986) relationship to calculate k since our study site was in a relatively fetch-limited area. Atmospheric CO_2 data were provided by CNR-ISAC and IAA (Consiglio Nazionale delle Ricerche Istituto di Scienze dell'Atmosfera e del Clima and Instituto Antártico Argentino), which continuously monitored CO_2 concentrations in air (mole fraction in dry air) over our sampling period at the neighbouring Jubany Station (62°14'S, 58°40'W). The atmospheric CO_2 concentration was converted to CO_2 fugacity in wet air using *in situ* sea surface temperature (SST) and salinity, air pressure, and humidity (Weiss 1974), giving a mean value of $368.6 \pm 5\,\mu$atm. Wind speed was measured at a height of $\sim 10\,m$ every 6 h from the *Sedna IV*'s meteorological station and daily averaged wind speed was used in the CO_2 flux calculation. Ice concentration data were provided by the National Snow and Ice Data Center (NSIDC) in Boulder, CO, USA (available at http://nsidc.org/data/nsidc-0051.html).

Results

General meteorology, hydrography, and biology

Air temperature ranged from -7 to 2°C (mean: -2.9°C; median: -4.0°C) during the study period with the coldest days occurring in late winter from 12 August–15 September (-5 to -7°C) and the warmest in late spring from 26 October– 10 November (0 to 2°C). Wind speed always remained below $10\,m\,s^{-1}$ (mean: $4.4\,m\,s^{-1}$; median: $3.6\,m\,s^{-1}$) except on 30 October during which wind speeds of 12.9–$15.5\,m\,s^{-1}$ were experienced (Fig. 2d). Excluding a few time windows in which total ice free conditions emerged, the study area was partially ice covered in the later half of the winter (28 July– 13 October) with ice concentration ranging from 7.6–69.2% and averaging 38.1%; the rest of the sampling season was completely ice free (Fig. 2f).

Water temperature showed a clear seasonal trend. Sea surface temperature (SST) ranged from -0.56 to -0.92°C (mean: -0.78°C) in late autumn (3–19 June), was close to the seawater freezing point throughout the winter (21 July–14 September), and started rising rapidly at the onset of the ice breakout on 14 October in spring (7 October–10 November) (Fig. 2b). SST reached the maximum of -0.04°C on the last sampling day (10 November). Seawater temperature increased with depth in the upper 120 m throughout the entire sampling period (Fig. 2b). The winter low-temperature tongue dominated the seasonal evolution of the water column temperature.
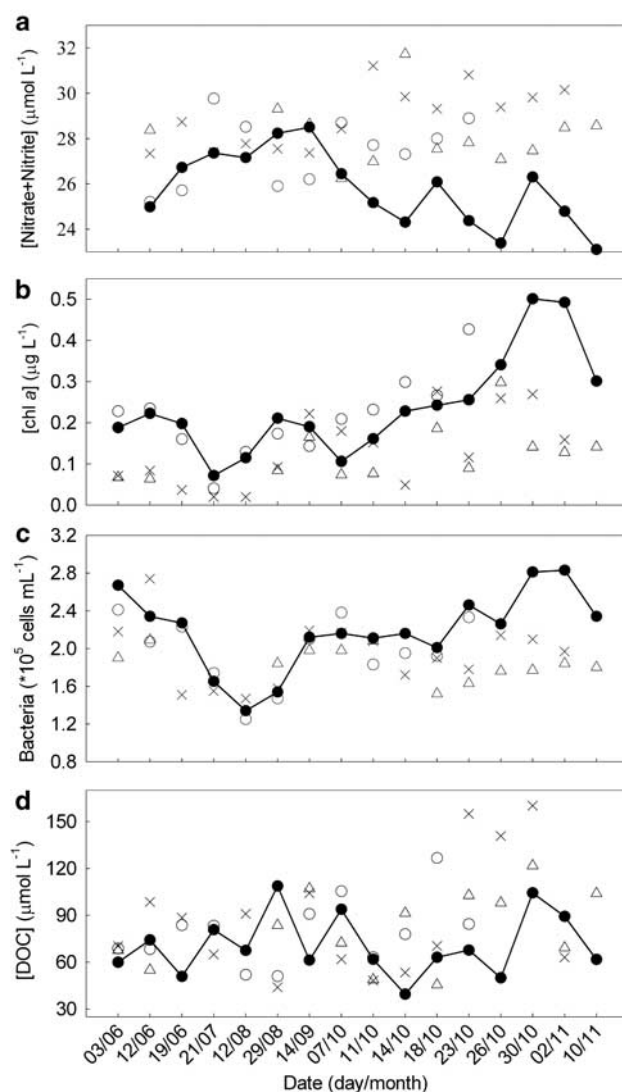

Fig. 3. Temporal variations of **a.** nitrate + nitrite, **b.** chl *a*, **c.** bacterial abundance, and **d.** DOC. Symbols are the same as those in Fig. 2a.

Salinity variation at the surface was small (33.8–34.07), being lower in late autumn and spring and higher in winter (Fig. 2c). The rapid drop of salinity starting on 7 October was probably due to ice melting. A 0.26 increase in salinity in late spring from 30 October–10 November followed the high wind speed observed on 30 October (Fig. 2d). Wind-driven mixing, therefore, probably caused the increase in salinity. Water column salinity structure was characterized by two large upward salty tongues separated by a minor downward fresher wedge in midwinter and overlain by two large downward fresher tongues formed in late autumn and late spring (data not shown). The largest salinity vertical gradients were recorded in late spring and the lowest in midwinter, exhibiting an opposing trend to that of the surface mixed-layer depth (ML_D), as determined by the $0.01\,kg\,m^{-3}$ difference criterion (Fig. 2e). The ML_D
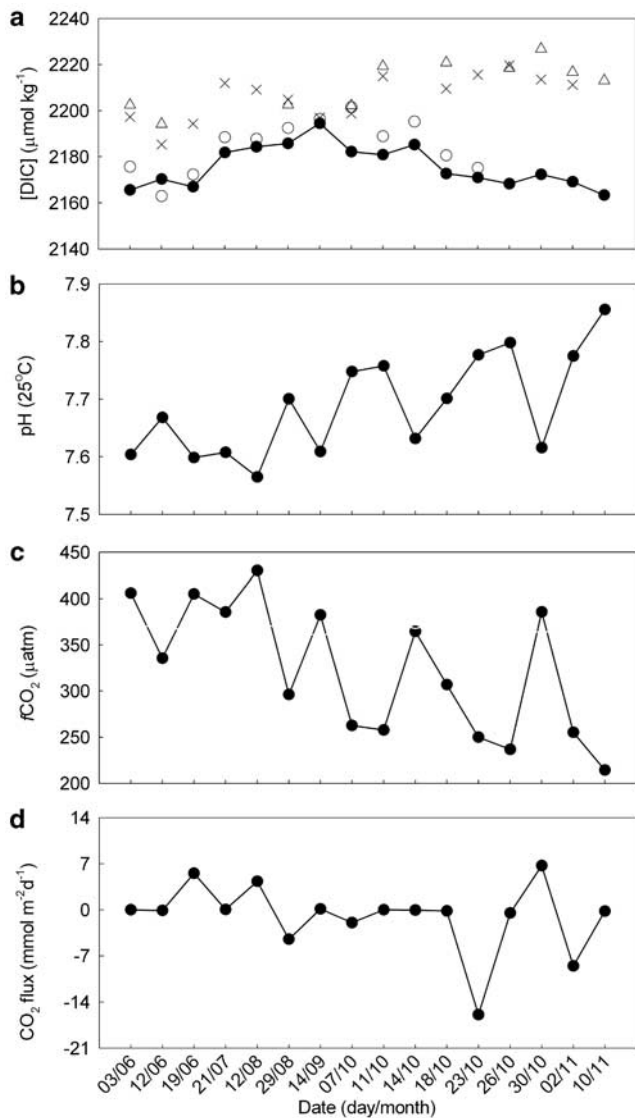
Fig. 4. Temporal variations of **a.** DIC, **b.** pH (25°C), **c.** $f\mathrm{CO_2}$ (filled circles and solid line = in seawater, grey line = in air), and **d.** $\mathrm{CO_2}$ flux. Symbols in panel **a** are the same as those in Fig. 2a.

increased slightly from late autumn (37.0 ± 20.3 m) to winter (40.0 ± 19.9 m) but shoaled to 10.4 ± 8.7 m in spring apparently due to surface warming (Fig. 2b) and ice melting-induced freshening (Fig. 2f). The deepening of the ML on 30 October echoed the high wind speeds at that time (Fig. 2e vs 2d) and supported the above argument on the concurrent rise in salinity.

Surface chl a was very low ($< 0.22 \, \mu g \, l^{-1}$) over the late autumn and winter periods (Fig. 3b). Slightly elevated chl a concentrations were observed during the first three sampling days and on 29 August and 14 September in late winter; the former possibly a remnant of higher chl a in early autumn while the latter could have resulted from phytoplankton production as daylength at that time lasted ~ 10 hr and ice concentrations were relatively low (Fig. 2f).

As expected from light-limited primary productivity, the sole under-ice water sample displayed a chl a minimum on 7 October. Accompanying the retreat of sea ice, chl a steadily increased from 11 October onward (Fig. 3b). The rapid drop of chl a at the end of the survey could be related to the wind-driven deepening of the ML as mentioned above. Vertically, subsurface chl a maxima occurred at times in spring but were mostly absent in late autumn and winter as expected (Fig. 3b).

Surface bacterial abundances were similar between spring ($2.4 \pm 0.3 \times 10^5$ cells ml^{-1}) and late autumn ($2.4 \pm 0.2 \times 10^5$ cells ml^{-1}) but winter's abundance was $c.$ 30% lower ($1.7 \pm 0.3 \times 10^5$ cells ml^{-1}). Temporal distribution of the surface bacterial abundance generally followed the seasonal trend of surface chl a (Fig. 3c vs 3b) and the two variables linearly correlated (R = 0.868) in spring. Subsurface bacterial abundances were usually lower than at the surface in late autumn and spring but little vertical variability was observed in winter (Fig. 3c).

Dissolved inorganic carbon

Surface DIC fell in a small range from 2163.3 to 2194.5 μmol kg^{-1} over the entire study period (Fig. 4a). Mean surface DIC increased from $2167.6 \pm 2.4 \, \mu$mol kg^{-1} in late autumn (3–19 June) to $2186.6 \pm 5.5 \, \mu$mol kg^{-1} in winter (21 July–14 September), and then decreased to $2173.8 \pm 7.2 \, \mu$mol kg^{-1} in spring (7 October–10 November). The highest surface DIC (2194.0 μmol kg^{-1}) was observed on 14 September in late winter (Fig. 4a). Surface DIC at our study site trended oppositely compared to water temperature (Fig. 4a vs Fig. 2b). The overall seasonal pattern of DIC was similar to that of salinity and inverse to that of chl a but the point-to-point correspondences were less consistent than those between DIC and T. Accordingly, the linear correlation of DIC vs T (R = -0.885) is better than those of DIC vs S (R = 0.561) and DIC vs chl a (R = -0.475). However, temperature-driven solubility variation could only account for < 4% of the maximum DIC variation in late autumn and winter (28.9 μmol kg^{-1}) and < 7% of that in spring (21.9 μmol kg^{-1}). The contribution from salinity-associated solubility change was negligible. On the other hand, as DIC generally increased with depth (Fig. 4a), the physical structure of the upper water column was expected to influence the surface DIC. Indeed, the difference in DIC between the bottom and surface of the sampled layer (ΔDIC) linearly correlated (R = 0.891) to the parallel difference in salinity over the whole sampling period; the correlation was better in late autumn and winter (R = 0.966) than in spring (R = 0.818). Additionally, the seasonal mean ΔDIC inversely varied with the seasonal mean ML$_D$: $29.4 \pm 6.7 \, \mu$mol kg^{-1} vs 37.0 m in late autumn, $17.9 \pm 13.1 \, \mu$mol kg^{-1} vs 40.0 m in winter, and $50.5 \pm 10.8 \, \mu$mol kg^{-1} vs 10.4 m in spring. Hence, weak stratifications and deepening of the ML brought warmer, saltier, and DIC-richer deeper water into the surface layer
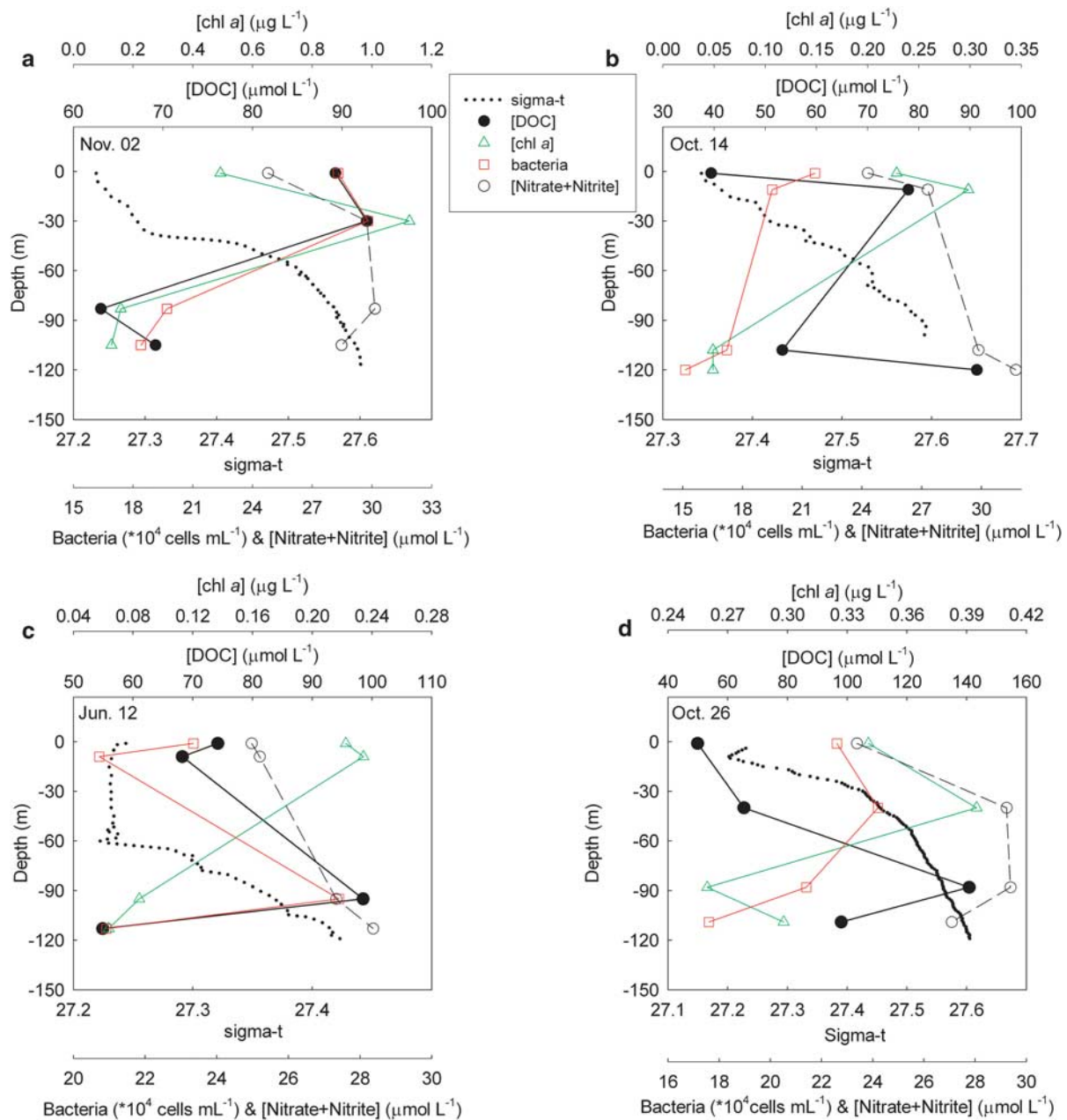
Fig. 5. Examples of vertical profiles of DOC, chl *a*, sigma-t, bacterial abundance, and nitrate + nitrite.

and thereby diminished the vertical DIC gradient in the ML. Increasing DIC with time over late autumn and winter should therefore principally be linked to the enhanced vertical mixing whereas the drawdown of DIC in spring was attributable to intensifying stratification of the upper layer along with growing primary production as indicated by chl *a* (Fig. 3b).

pH

Surface pH ranged from 7.57–7.86 over the sampling period with the highest pH values (> 7.8) recorded in late

spring when chl *a* concentrations were relatively elevated (Fig. 4b). Mean pH was lower in late autumn and winter (7.62 ± 0.05) than in spring (7.74 ± 0.08), conforming to the seasonal trend of the mean chl *a*: $0.17 \pm 0.06 \, \mu g \, l^{-1}$ in late autumn and winter vs $0.29 \pm 0.14 \, \mu g \, l^{-1}$ in spring. However, on a point-to-point basis, pH correlated better with nitrate + nitrite ($R = -0.698$) than with chl *a* ($R = 0.335$), implying that net community production, which accounts for heterotrophic respiration, rather than primary production alone, controlled pH. Rising temperature in spring also affected pH but contributed only *c*. 10% of the observed change.

Fugacity and air-sea flux of CO₂

Surface water $f\text{CO}_2$ ranged from 214.0 µatm on 10 November in spring to 430.0 µatm on 12 August in winter and averaged 323.5 ± 71 µatm (Fig. 4c). CO_2 at the surface was generally supersaturated relative to atmospheric CO_2 in late autumn and winter (377.4 ± 46 µatm) but undersaturated in spring (281.5 ± 58 µatm). The CO_2 saturation state rendered our study site to be a weak CO_2 source for the atmosphere in late autumn and winter (mean FCO₂: $0.78 \text{ mmol m}^{-2} \text{ d}^{-1}$) and a moderate sink in spring (mean FCO₂: $-2.3 \text{ mmol m}^{-2} \text{ d}^{-1}$) (Fig. 4d). In spring FCO₂ varied widely from day to day, keeping in-line with the corresponding fluctuations of the wind speed (Fig. 2d). Winter FCO₂ values could be overestimates as the study area was usually partially ice covered in that season (Fig. 2f).

Dissolved organic carbon

Surface DOC varied between 39.4 (14 October) and $108.6 \text{ µmol l}^{-1}$ (29 August) and averaged $70.9 \pm 19.7 \text{ µmol l}^{-1}$ over the entire sampling period. No consistent temporal DOC trends were observed at the surface and depth (Fig. 3d). Seasonally averaged surface DOC increased from $61.6 \pm 11.7 \text{ µmol l}^{-1}$ in late autumn to $79.5 \pm 21.1 \text{ µmol l}^{-1}$ in winter and then decreased slightly to $70.1 \pm 21.3 \text{ µmol l}^{-1}$ in spring. The depth-weighted mean DOC in the ML, defined as the DOC inventory in the upper ML divided by the ML$_D$, over the whole sampling period ranged from $51.0–107.6 \text{ µmol l}^{-1}$ and averaged $75.4 \pm 15.0 \text{ µmol l}^{-1}$.

The vertical distribution of DOC in the water column was complicated with patches of high DOCs located at varying layers below the surface ML. Figure 5 illustrates various types of vertical structures of DOC. DOC profiles on 3 June, 18 and 23 October, 2 November resembled the corresponding chl *a* profiles (Fig. 5a), suggesting a close linkage between DOC formation and primary production at these times. Similar correspondences were also found for 29 August, 7, 11 and 14 October except at the deepest sampling depths where the chl *a* and DOC distributions diverged (Fig. 5b). Some profiles of DOC were similar to those of heterotrophic bacterial abundance (12 June, 21 July, 12 and 29 August, 2 November; Fig. 5c) and/or to those of nitrate + nitrite (21 July, 23, 26 and 29 August, 30 October, 10 November; Fig. 5d), pointing to DOC as an important substrate for bacterial multiplication and nutrient production from remineralization of dissolved organic matter.

Discussion

This section compares our results with those from previous studies, assesses the biological and physical processes regulating $f\text{CO}_2$ and DIC, discusses the implication of DOC dynamics, and evaluates the fate of net community production that was derived from mass-balance budgeting of DIC.

Comparison with previous studies

Our spring's chl *a* concentrations are far below the reported chl *a* concentrations ($> 1 \text{ µg l}^{-1}$) during phytoplankton blooms in the adjacent Bellingshausen Sea and Gerlache Strait, which usually occur in the summer season (Álvarez *et al.* 2002, Carrillo *et al.* 2004, Ducklow *et al.* 2007). Bacterial abundances in autumn and spring from the present study are smaller than the summer's values obtained in the Bellingshausen Sea ($3.2 \times 10^5 \text{ cells ml}^{-1}$) and Gerlache Strait ($3.8–5.7 \times 10^5 \text{ cells ml}^{-1}$) (Vaqué *et al.* 2002) and in the shelf waters south-west off Anvers Island ($3.8 \times 10^5 \text{ cells ml}^{-1}$) (Church *et al.* 2003). Our winter value is, however, three times the winter's bacterial abundance ($0.6 \times 10^5 \text{ cells ml}^{-1}$) reported for the shelf waters south-west off Anvers Island (Church *et al.* 2003). The DIC values observed in the present study lie in the summer–winter DIC range in surface waters west of our study site (Carrillo *et al.* 2004) and in the annual DIC variation limits in Prydz Bay, East Antarctica (Gibson & Trull 1999). Our mean $f\text{CO}_2$ in spring is within the range of the summer's mean $f\text{CO}_2$ values (241–313 µatm) reported for the adjacent Bellingshausen Sea and Gerlache Strait (Álvarez *et al.* 2002). The supersaturation observed in winter at our site is consistent with previous results obtained in other Antarctic surface waters (Takahashi *et al.* 1993, Carrillo & Karl 1999, Gibson & Trull 1999, Carrillo *et al.* 2004). Our mean winter supersaturation (2%) is however, lower than that (10%) in the area west off Anvers Island (Carrillo *et al.* 2004). The spring's mean CO_2 influx calculated by the present study is below the summer's mean influxes ($3.8–15.9 \text{ mmol m}^{-2} \text{ d}^{-1}$) in the Bellingshausen Sea and Gerlache Strait (Álvarez *et al.* 2002), in accordance with the higher phytoplankton biomass observed by the latter authors. It should be noted that our CO_2 flux estimates (absolute values) would increase approximately by a factor of two if the Wanninkhof (1992)'s formulation were used to calculate the piston velocity. Surface DOCs at our study site are within the DOCs in coastal Antarctic waters reported by Gibson (1998) and Hansell & Carlson (1998) ($41.7–185 \text{ µmol l}^{-1}$) and by Scott *et al.* (2000) ($30.0–258.3 \text{ µmol l}^{-1}$). The complex vertical structures of DOC found here are consistent with the observations by Dafner (1992) and Doval *et al.* (2002) in other Antarctic waters. The increasing DOC at the bottom of some profiles (Fig. 5b) was probably due to a DOC input from the underlying sediment as suggested by Doval *et al.* (2002).

Processes controlling fCO₂

The slight CO_2 supersaturation ($4 \pm 11\%$) in late autumn could largely result from bacterial respiration as evidenced by the relatively high bacterial abundance then (Fig. 3c). The fairly high SST ($-0.78 \pm 0.2°\text{C}$) at that time should also play a role in creating this supersaturation. In winter 50% (8.8 µatm) of the decrease in $f\text{CO}_2$ from 19 June (T: $-0.87°\text{C}$; $f\text{CO}_2$: 405.3 µatm) to 21 July (T: $-1.46°\text{C}$; $f\text{CO}_2$: 385.7 µatm) could be accounted

Table I. Seasonally averaged values of the total dissolved inorganic carbon (TDIC), the Revelle factor (β), the observed change of $f\mathrm{CO_2}$ ($\Delta f/\Delta t$), the thermodynamic change ($[\delta f/\delta t]_T$), the air-sea exchange ($[\delta f/\delta t]_F$), and the residual term ($[\delta f/\delta t]_R$) as defined in Eqs (2) & (3).

	Δt (d)	TDIC (mol m^{-2})	β	$\Delta f/\Delta t$ (μatm d^{-1})	$[\delta f/\delta t]_T$ (μatm d^{-1})	$[\delta f/\delta t]_F$ (μatm d^{-1})	$[\delta f/\delta t]_R$ (μatm d^{-1})
Late autumn and winter (3 June–14 Sept)	103	86.85	15.56	0.17	-0.2	-0.08	0.45
Spring (7 Oct–10 Nov)	34	30.54	15.5	-2.95	0.77	0.81	-4.52

for by surface cooling based on calculation using the temperature coefficient of $f\mathrm{CO_2}$ in seawater (4.23% °C^{-1} or c. 15 μatm, Takahashi *et al*. 1993). The surprising $\mathrm{CO_2}$ undersaturation on 29 August (by 20%, 72.3 μatm) could result from a combination of the cooling effect, diminished air-sea exchange, weak respiration, and $\mathrm{CO_2}$ uptake by phytoplankton production as inferred from decreasing water temperature, ice cover, low bacterial abundance, and elevated chl *a* (Figs 2 & 3) and phytoplankton cell abundance (S. Moreau *et al*. unpublished) at that time. The $\mathrm{CO_2}$ undersaturation in spring was apparently due mainly to enhanced biological $\mathrm{CO_2}$ uptake in the water column. However, the low $f\mathrm{CO_2}$ values for the first two spring sampling days (i.e. 7 and 11 October) (Fig. 4c), when the area was still partially ice covered (Fig. 2f), were not expected from the low surface-water chl *a* concentrations (Fig. 3b) but were supported by the drawdown of nitrate + nitrite (Fig. 3a) at the corresponding times. This seeming paradox might have resulted from the uptake of water column $\mathrm{CO_2}$ and nutrients by microalgae growing in the bottom sea ice, as previously observed by Lee *et al*. (2008). Ice algae blooms usually precede water column phytoplankton blooms by a couple of months (Fritsen *et al*. 2008), which fits the timeline for an ice algae bloom in early spring at our site (water column bloom there often starts in early summer). Direct observations by divers of the *Sedna IV* expedition confirmed profuse colonization of microalgae in sea ice at this time of the year in the sampling area.

More quantitatively, processes controlling the temporal evolution of surface $f\mathrm{CO_2}$ were evaluated according to the

equation of Bakker *et al*. (1997):

$$\Delta f/\Delta t = [\delta f/\delta t]_T + [\delta f/\delta t]_F + [\delta f/\delta t]_R \qquad (2)$$

$\Delta f/\Delta t$ is the observed change of $f\mathrm{CO_2}$ in the time interval of Δt, which is the sum of variations in $f\mathrm{CO_2}$ due to thermodynamic changes ($[\delta f/\delta t]_T$), air-sea exchange ($[\delta f/\delta t]_F$), and a residual term ($[\delta f/\delta t]_R$) representing the combined effects of biological activity and physical processes other than temperature and salinity variations (e.g. vertical mixing). $[\delta f/\delta t]_T$ was calculated using the $\mathrm{CO_2}$-system programme by Lewis & Wallace (1998) and $[\delta f/\delta t]_F$ using Bakker *et al*.'s (1997) equation:

$$[\delta f/\delta t]_F = F_{av} \, \beta f\mathrm{CO_2}^{av} \, \mathrm{TDIC}^{-1} \qquad (3)$$

F_{av} and $f\mathrm{CO_2}^{av}$ are, respectively, the average $\mathrm{CO_2}$ flux and surface $f\mathrm{CO_2}$ over Δt, β, the Revelle factor (i.e. $\delta\ln(f\mathrm{CO_2})/\delta\ln\mathrm{DIC}$), and TDIC the product of the mean depth-weighted DIC in the ML, the $\mathrm{ML_D}$, and the seawater density at the start of each Δt (Bakker *et al*. 1997). Subtracting $[\delta f/\delta t]_T$ and $[\delta f/\delta t]_F$ from the observed $\Delta f/\Delta t$ gives the residual term, $[\delta f/\delta t]_R$. Each term in Eq. (2) was calculated for Δt corresponding to each time interval (days) between two adjacent sampling days. Seasonal mean values of these terms (Table I) were obtained by averaging the two-point-based values for each specific season. The mean relative error for $\Delta f/\Delta t$, $[\delta f/\delta t]_T$, $[\delta f/\delta t]_F$, and $[\delta f/\delta t]_R$ in Eq. (2) was estimated to be $\pm 31\%$, $\pm 41\%$, $\pm 48\%$, and $\pm 23\%$.

In late autumn and winter the residual term, supposedly due largely to respiration and vertical mixing, raised $f\mathrm{CO_2}$ by 0.45 μatm d^{-1} while surface cooling and outgassing drew down $f\mathrm{CO_2}$ by 0.20 and 0.08 μatm d^{-1}, respectively, leading to a net $f\mathrm{CO_2}$ increase of 0.17 μatm d^{-1}. In contrast, the springtime residual term, to which primary production was likely the main contributor, reduced $f\mathrm{CO_2}$ by 4.52 μatm d^{-1}. This $\mathrm{CO_2}$ drawdown was partially offset by vernal surface warming and atmospheric $\mathrm{CO_2}$ input, which increased $f\mathrm{CO_2}$ by 0.77 and 0.81 μatm d^{-1}, respectively, giving rise to a net $f\mathrm{CO_2}$ decrease of 2.95 μatm d^{-1}. In both periods the residual term was the main control on the $f\mathrm{CO_2}$ variation while gas exchange and thermodynamic changes were much less important.

Mass-balance budgeting for DIC

Figure 6 displays DIC as a function of nitrate + nitrite in the upper ML on a salinity-normalization basis, which is
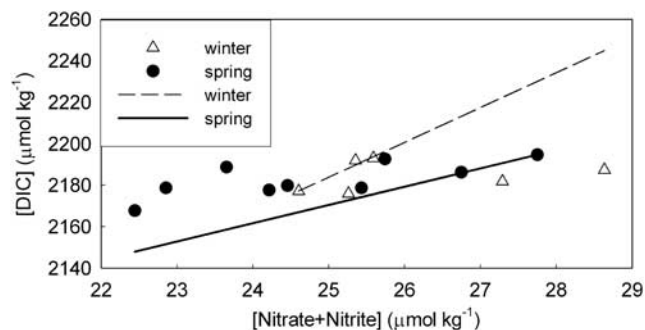

Fig. 6. Plot of DIC vs nitrate + nitrite in the upper mixed layer. Lines indicate DIC expected from nitrate and nitrite uptake and the POC:PON ratios determined in this study (see text). The starting DIC was set at 2236.6 μmol l^{-1} for winter and 2254.9 μmol l^{-1} for spring. Both DIC and nitrate + nitrite are normalized to salinity 34.

Table II. Seasonally averaged changes in salinity-normalized DIC from observation (ΔDIC_{obs}), biological activity (ΔDIC_{bio}), vertical mixing (ΔDIC_{mix}), and air-sea exchange (ΔDIC_{exch}) as defined in Eq. (4).

	ΔDIC_{obs} (mmol m^{-2} d^{-1})	ΔDIC_{bio} (mmol m^{-2} d^{-1})	ΔDIC_{mix} (mmol m^{-2} d^{-1})	ΔDIC_{exch} (mmol m^{-2} d^{-1})
Late autumn and winter (3 June–14 Sept)	4.7	5.1	0.4	0.8
Spring (7 Oct–10 Nov)	-12.6	-19.3	1.4	-5.3

intended to eliminate the effect of dilution by melting sea ice. The measured data points for winter and spring are mostly below and above, respectively, the theoretical lines predicted from the concurrently measured molar ratios of particulate organic carbon (POC) to particulate organic nitrogen (PON), 16.8 ± 3.2 for winter and 8.8 ± 1.0 for spring (E. Pelletier *et al.* unpublished data). Our winter POC:PON ratios are close to those observed by Carlson *et al.* (2000) and Hansell & Carlson (2001). This pattern indicates a net loss of DIC in the upper ML in winter and a net gain in spring due to processes other than biological activity. The loss of DIC in winter could result from efflux of CO_2 to the atmosphere while the gain in spring could be a consequence of atmospheric CO_2 influx and upward DIC diffusion from below the ML. The scattering of the data reflects the variability of these processes over the sampling period.

A mass-balance model, modified from Bégovic & Copin-Montégut (2002) and Fransson *et al.* (2004), was employed to quantitatively assess the relative importance of different processes in controlling the seasonal dynamics of DIC. Neglecting horizontal advection (as it is unknown), we can express the model as:

$$\Delta DIC_{obs} = \Delta DIC_{bio} + \Delta DIC_{exch} + \Delta DIC_{mix} \qquad (4)$$

where ΔDIC_{obs}, ΔDIC_{bio}, ΔDIC_{exch}, and ΔDIC_{mix} represent the change in salinity-normalized DIC (salinity 34) from observation, biological activity, air-sea exchange, and vertical mixing, respectively. The model was applied to the upper mixed layer and two seasons: winter including late autumn (3 June–14 September) and spring (7 October–10 November). ΔDIC_{bio} was calculated as the product of nitrate and nitrite uptake or release and the measured molar POC:PON ratios from this study. ΔDIC_{mix} was estimated by multiplying vertical eddy diffusivity, K_z, by dDIC/dz between ML_D and 100 m using a K_z value of 3×10^{-5} m^2 s^{-1} (De Baar *et al.* 1995, Bakker *et al.* 1997, Álvarez *et al.* 2002). ΔDIC_{exch} was then computed as ΔDIC_{obs} - ΔDIC_{bio} - ΔDIC_{mix}. Results are shown in Table II. The mean relative error for ΔDIC_{obs}, ΔDIC_{bio}, ΔDIC_{exch}, and ΔDIC_{mix} in Eq. (4) was estimated to be $\pm$ 49%, $\pm$ 19%, $\pm$ 27%, and $\pm$ 11% in winter, and $\pm$ 14%, $\pm$ 11%, $\pm$ 34%, and $\pm$ 7% in spring. ΔDIC_{bio} approximates bacterial remineralization in winter due to weak primary production at that time and corresponds to net community production in spring. Clearly, biological activity dominated over air-sea exchange and vertical transport in regulating the dynamics of DIC in both seasons. As expected, the study area acted as a source of CO_2 in winter and a sink in spring. The air-sea flux

term was more than twice the vertical mixing term in both seasons. Note that we did not take into account the change in DIC due to biological calcium carbonate since the cell abundance of calcareous organisms during our study period was undetectable (S. Moreau *et al.* unpublished).

Qualitatively, the CO_2 flux derived from the mass-balance model is in the same direction (i.e. source in winter and sink in spring) as that for the flux based on fCO_2 and piston velocities. Quantitatively, the former is similar to the latter (0.80 vs 0.78 mmol m^{-2} d^{-1}) in winter but more than twice the latter (-5.3 vs -2.3 mmol m^{-2} d^{-1}) in spring. Given the two-fold uncertainty in the piston velocity calculation and the further complication by ice coverage, these two independent approaches actually reach a reasonable agreement. This concord indirectly validates the assumption made in the mass-balance model, i.e. insignificant horizontal advection.

Based on the observation of strong summertime CO_2 undersaturation in the north-east water polynya on the Greenland Shelf, Yager *et al.* (1995) hypothesized that marginal sea ice zones in the Arctic Ocean act as a rectified (one-way) net annual CO_2 sink that provides a negative feedback to increasing atmospheric CO_2. A key assumption underlying this hypothesis is that air-sea gas exchange is effectively blocked by sea ice in winter and by intense surface stratification in spring due to freshening of the water column by sea ice melting. Consequently, DIC accumulated in the water column during winter cannot be transferred to the atmosphere via gas exchange before it is consumed by primary production in spring. In the present study, however, escape of CO_2 to the atmosphere in winter was not completely prevented due to only partial ice coverage, as also observed in other WAP marginal sea ice zones (e.g. Carrillo *et al.* 2004). Furthermore, summertime surface water CO_2 in the WAP shelf region can be near atmospheric equilibrium or supersaturation, instead of undersaturation, (Álvarez *et al.* 2002, Carrillo *et al.* 2004). Therefore, the Scholaert Channel and some other WAP coastal and shelf areas probably do not act as a rectified CO_2 sink. As the WAP is one of the most rapidly warming regions on Earth (Ducklow *et al.* 2007), this leads to a broader implication in relation to whether climate warming strengthens the rectified sink, if it does exist. Yager *et al.* (1995) suggested that rising temperature increases the seasonally ice covered area and thus the rectified sink as well. Yet rising temperature also reduces the concentration and thickness of sea ice, which diminishes the effectiveness of sea ice as a barrier for air-sea gas exchange. Moreover, the contraction of sea ice leads to
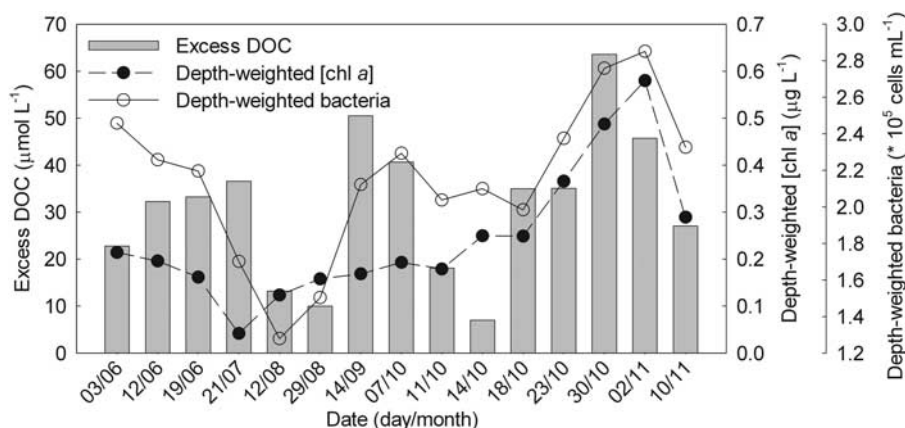
Fig. 7. Temporal variations of depth-weighted mean excess DOC, chl *a*, and bacterial abundance in the surface mixed layer.

less freshening (thus less stratification) of the water column once sea ice melts, thereby facilitating CO_2 exchange to air through wind-driven mixing in early spring when CO_2 is well above atmospheric equilibrium. Hence, the impacts of climate warming on the dynamics of DIC in relation to the rectified sink hypothesis appear rather complex. In fact, the most recent flux estimation by Takahashi *et al.* (2009) demonstrates that the Antarctic marginal sea ice zones are a weak source, instead of sink, of atmospheric CO_2.

Implication of DOC dynamics

Our DOC data indicate an excess of DOC in the surface ML against a deepwater background DOC of 44 μmol l^{-1} found by Doval *et al.* (2002) in the vicinity of our sampling site or of 39 μmol l^{-1} obtained by Ducklow *et al.* (2007) in a more extensive WAP shelf region. The former was adopted for calculating the excess DOC in the present study, giving mean excess DOC values of 29.4 ± 5.8 μmol l^{-1} in late autumn, 27.6 ± 19.4 μmol l^{-1} in winter, and 34.0 ± 17.3 μmol l^{-1} in spring. The overall range of the excess DOC (7.0–63.6 μmol l^{-1}) from this study indicates that 14–59% (mean: 39%) of the measured DOC in the ML of the sampling site was labile or semi-labile. This large variability of excess DOC is consistent with the observations by Doval *et al.* (2002) in the adjacent area in summer (15–57%) and by Hansell & Peltzer (1998) in the Arabian Sea (31–58%). Using the concurrently determined particulate organic carbon concentration (POC) (E. Pelletier *et al.* unpublished data), we calculated the ratio of excess DOC to excess DOC plus POC. This ratio showed little intra- and inter-seasonal variability and averaged 79 ± 10% for the entire sampling period, indicating that 79% of the potentially degradable organic carbon existed in dissolved form and 21% as suspended particles. Our ratio is larger than the summertime ratio of 59% in the nearby Bransfield and Gerlache straits (Doval *et al.* 2002) but comparable to the ratio of 89% in the Mediterranean Sea (Copin-Montégut & Avril 1993).

The seasonal pattern of the excess DOC generally followed that of the depth-weighted mean chl *a* in the ML (Fig. 7), indicating that primary production was a key control on the accumulation of DOC. Considering the low phytoplankton biomass in late autumn and winter, we suspect that the excess DOC at that time could be a remnant of DOC accumulated during the preceding summer phytoplankton bloom. Our higher DOC excess value in spring agrees with the findings by Copin-Montégut & Avril (1993) and Carlson *et al.* (1994) for warmer seas. The springtime increase in the excess DOC indicated that phytoplankton-based DOC production overtook DOC losses due to vertical and horizontal DOC transport and bacterial remineralization which should also be enhanced in spring as inferred from the higher bacterial abundance in the ML (Fig. 7). The similar temporal trends of the bacterial abundance and excess DOC (Fig. 7) further demonstrate that DOC was plausibly the main substrate for bacterial growth during the sampling period.

Fate of net community production

In spring, the biological term in Eq. (4), ΔDIC_{bio}, represents the net community production at the study site given by

$$\Delta DIC_{bio} = \Delta POC + \Delta DOC + E \qquad (5)$$

where ΔPOC and ΔDOC are the measured changes in the concentrations of POC and DOC in the upper ML in spring (11 October–10 November), and E the downward flux of POC that can be estimated as ΔDIC_{bio} - ΔPOC - ΔDOC. The values of ΔPOC, ΔDOC, and E are 0.8 ± 0.1, 3.6 ± 1.3, and 2.9 ± 1.4 mmol m^{-2} d^{-1}, respectively, accounting for 11, 50, and 39% of ΔDIC_{bio} (7.3 ± 0.3). Therefore, DOC production is the dominant fate of the net community production, followed by the downward transport of POC, and biomass increase. The similarity in the patterns of temporal distributions of DOC and chl *a* in spring (Fig. 7) suggests that extracellular release could be mainly responsible for DOC production. The percent ΔDOC value from this study is at the

upper end of the summertime percent extracellular release range reported by Morán & Estrada (2002) for the nearby Bransfield and Gerlache straits (3–47%) and within the range reported by Gosselin *et al*. (1997) for the Canada Basin in the Arctic Ocean (31–65%). This high percent ΔDOC value might be related to enhanced extracellular DOC release under high doses of UV-B radiation as a result of the Antarctic springtime ozone hole that occurred over our sampling period (Carrillo *et al*. 2006, S. Moreau et al. unpublished). The downward export term from our study is much lower than the summertime values obtained by Álvarez *et al*. (2002) for the adjacent Bellingshausen Sea ($9.0\,mmol\,m^{-2}\,d^{-1}$) and Gerlache Strait ($23.5\,mmol\,m^{-2}\,d^{-1}$), in accordance with the lower phytoplankton production at our sampling time. The difference in the percent E value between the two studies is, however, smaller: 39% vs 67% (for the Gerlache Strait).

Conclusions

This study examined the seasonal evolution of water-column DIC, DOC, and related meteorological, physical, biological, chemical variables at a coastal water site off the West Antarctic Peninsula. Surface DIC spanned a small range (2163.3 to $2194.5\,\mu mol\,kg^{-1}$) and increased from late autumn to winter and then decreased in spring. No consistent temporal trends of DOC were observed but an excess of DOC ($7.0–63.6\,\mu mol\,l^{-1}$) existed in the surface ML throughout the sampling period. Mass-balance modelling was employed to assess the relative importance of various processes in controlling the seasonal DIC dynamics and in the partition of the net community production in spring. Despite the very low biomass of both autotrophic and heterotrophic organisms, the biological contribution to the DIC dynamics was considerably higher than those from air-sea exchange and physical mixing. The net community production in spring was mainly funnelled through DOC and sinking particles rather than suspended POC in the upper ML. CO_2 at the surface was slightly supersaturated (by 2%) in late autumn and winter and moderately undersaturated (by 24%) in spring. Both mass-balance modelling and fCO_2-based calculation indicate that the study area was a source of CO_2 to the atmosphere in late autumn and winter ($\sim0.8\,mmol\,m^{-2}\,d^{-1}$) and a sink in spring ($2.3–5.3\,mmol\,m^{-2}\,d^{-1}$). The Scholaert Channel will probably not act as a rectified (one-way) annual CO_2 sink in the context of climate warming. More surveys are needed to consolidate these conclusions and to verify their applicability to other Antarctic coastal and shelf regions owing to the relatively sparse wintertime sampling resolution in our study and to large inter-annual and spatial variability of the Antarctic marine ecosystems, including ice coverage.

References

Álvarez, M., Ríos, A.F. & Rosón, G. 2002. Spatio-temporal variability of air-sea fluxes of carbon dioxide and oxygen in the Bransfield and Gerlache Straits during austral summer 1995–96. *Deep-Sea Research II*, **49**, 643–662.

Bakker, D.C.E., De Baar, H.J.W. & Bathmann, U.V. 1997. Changes of carbon dioxide in surface waters during spring in the Southern Ocean. *Deep-Sea Research II*, **44**, 91–127.

Bégovic, M. & Copin-Montégut, C. 2002. Processes controlling annual variations in the partial pressure of CO_2 in surface waters of the central northwestern Mediterranean Sea (Dyfamed site). *Deep-Sea Research II*, **49**, 2031–2047.

Bertolin, M.L. & Schloss, I.R. 2009. Phytoplankton production after the collapse of the Larsen A Ice Shelf, Antarctica. *Polar Biology*, 10.1007/s00300-009-0638-x.

Cai, W.J. & Wang, Y. 1998. The chemistry, fluxes, and sources of carbon dioxide in the estuarine waters of the Satilla and Altamaha rivers, Georgia. *Limnology and Oceanography*, **43**, 657–668.

Carlson, C.A. 2002. Production and removal processes. *In* Hansell, D.A & Carlson, C.A., *eds. Biogeochemistry of marine dissolved organic matter*. San Diego, CA: Academic Press, 91–139.

Carlson, C.A., Ducklow, H.W. & Michaels, A.F. 1994. Annual flux of dissolved organic-carbon from the euphotic zone in the northwestern Sargasso Sea. *Nature*, **371**, 405–408.

Carlson, C.A., Hansell, D.A., Peltzer, E.T. & Smith, W.O. 2000. Stocks and dynamics of dissolved and particulate organic matter in the southern Ross Sea, Antarctica. *Deep-Sea Research II*, **47**, 3201–3225.

Carrillo, C.J. & Karl, D.M. 1999. Dissolved inorganic carbon pool dynamics in northern Gerlache Straits, Antarctica. *Journal of Geophysical Research-Oceans*, **104**, 15873–15884.

Carrillo, C.J., Smith, R.C. & Karl, D.M. 2004. Processes regulating oxygen and carbon dioxide in surface waters west of the Antarctic Peninsula. *Marine Chemistry*, **84**, 161–179.

Carrillo, P., Medina-Sánchez, J.M., Villar-Argaiz, M., Delgado-Molina, J.A. & Bullejos, F.J. 2006. Complex interactions in microbial food webs: stoichiometric and functional approaches. *Limnetica*, **25**, 189–204.

Chen, F., Cai, W.J., Wang, Y., Rii, Y.M., Bidigare, R.R. & Benitez-Nelson, C.R. 2008. The carbon dioxide system and net community production within a cyclonic eddy in the lee of Hawaii. *Deep-Sea Research. II*, **55**, 1412–1425.

Church, M.J., DeLong, E.F., Ducklow, H.W., Karner, M.B., Preston, C.M. & Karl, D.M. 2003. Abundance and distribution of planktonic Archaea and Bacteria in the waters west of the Antarctic Peninsula. *Limnology and Oceanography*, **48**, 1893–1902.

Copin-Montégut, G. & Avril, B. 1993. Vertical distribution and temporal variation of dissolved organic carbon in the north-western Mediterranean Sea. *Deep-Sea Research*, **40**, 1963–1972.

DAFNER, E.V. 1992. Dissolved organic-carbon in waters of the Polar Frontal Zone of the Atlantic Antarctic in the spring summer season of 1988–1989. *Marine Chemistry*, **37**, 275–283.

DAVIDSON, A.T. & MARCHANT, H.J. 1992. Protist abundance and carbon concentration during a phaeocystis-dominated bloom at an Antarctic coastal site. *Polar Biology*, **12**, 387–395.

DE BAAR, H.J.W., DE JONG, J.T.M., BAKKER, D.C.E., LÖSCHER, B.M., VETH, C., BATHMANN, U. & SMETACEK, V. 1995. Importance of iron for plankton blooms and carbon dioxide drawdown in the Southern Ocean. *Nature*, **373**, 412–415.

DOVAL, M.D., ÁLVAREZ-SALGADO, X.A., CASTRO, C.G. & PÉREZ, F.F. 2002. Dissolved organic carbon distributions in the Bransfield and Gerlache Straits, Antarctica. *Deep-Sea Research II*, **49**, 663–674.

DUCKLOW, H.W., BAKER, K., MARTINSON, D.G., QUETIN, L.B., ROSS, R.M., SMITH, R.C., STAMMERJOHN, S.E., VERNET, M. & FRASER, W. 2007. Marine pelagic ecosystems: the West Antarctic Peninsula. *Philosophical Transactions of the Royal Society*, **B362**, 67–94.

FRITSEN, C.H., MEMMOTT, J. & STEWART, F.J. 2008. Inter-annual sea-ice dynamics and micro-algal biomass in winter pack ice of Marguerite Bay, Antarctica. *Deep-Sea Research II*, **55**, 2059–2067.

FRANSSON, A., CHIERICI, M., ANDERSON, L.G. & DAVID, R. 2004. Transformation of carbon and oxygen in the surface layer of the eastern Atlantic sector of the Southern Ocean. *Deep-Sea Research II*, **51**, 2757–2772.

GARCÍA, M.A., CASTRO, C.G., RÍOS, A.F., DOVAL, M.D., ROSÓN, G., GOMIS, D. & LÓPEZ, O. 2002. Water masses and distribution of physico-chemical properties in the Western Bransfield Strait and Gerlache Strait during Austral summer 1995/96. *Deep-Sea Research II*, **49**, 585–602.

GIBSON, J.A.E. 1998. Carbon flow through inshore marine environments of the Vestfold Hills, East Antarctica. *ANARE Scientific Reports*, no. 139, 224 pp.

GIBSON, J.A.E. & TRULL, T.W. 1999. Annual cycle of f_{CO_2} under sea-ice and in open water in Prydz Bay, East Antarctica. *Marine Chemistry*, **66**, 187–200.

GRASSHOF, K., EHRAHRDT, M. & KREMLING, K. 1983. *Methods of seawater analysis*, 2nd ed. Weinheim, Germany: Verlag Chemie, 419pp.

GOSSELIN, M., LEVASSEUR, M., WHEELER, P.A., HORNER, R.A. & BOOTH, B.C. 1997. New measurements of phytoplankton and ice algal production in the Arctic Ocean. *Deep-Sea Research II*, **44**, 1623–1644.

HANSELL, D.A. & CARLSON, C.A. 1998. Deep-ocean gradients in the concentration of dissolved organic carbon. *Nature*, **395**, 263–266.

HANSELL, D.A. & CARLSON, C.A. 2001. Biogeochemistry of total organic carbon and nitrogen in the Sargasso Sea: control by convective overturn. *Deep-Sea Research II*, **48**, 1649–1667.

HANSELL, D.A. & PELTZER, E.T. 1998. Spatial and temporal variations of total organic carbon in the Arabia Sea. *Deep-Sea Research II*, **45**, 2171–2193.

HOPPEMA, M., STOLL, M.H.C. & DE BAAR, H.J.W. 2000. CO_2 in the Weddell Gyre and Antarctic Circumpolar Current: austral autumn and early winter. *Marine Chemistry*, **72**, 203–220.

HOPPEMA, M., FAHRBACH, E., SCHRÖDER, M., WISOTZKI, A. & DE BAAR, H.J.W. 1995. Winter-summer differences of carbon dioxide and oxygen in the Weddell Sea surface layer. *Marine Chemistry*, **51**, 177–192.

LEE, S.H., WHITLEDGE, T.E. & KANG, S.H. 2008. Spring time production of bottom ice algae in the landfast sea ice zone at Barrow, Alaska. *Journal of Experimental Marine Biology and Ecology*, **367**, 204–212.

LEWIS, E. & WALLACE, D.W.R. 1998. *Program Developed for CO_2 system calculations*. Oak Ridge, TN: Oak Ridge National Laboratory, ORNL/CDIAC-105.

LISS, P.S. & MERLIVAT, L. 1986. Air-sea exchange rates: Introduction and synthesis. *In* BUAT-MENARD, P., *ed. The role of air-sea exchange in geochemical cycling*. Dordrecht: Reidel, 113–127.

METZL, N. 2009. Decadal increase of oceanic carbon dioxide in Southern Indian Ocean surface waters (1991–2007). *Deep-Sea Research II*, **56**, 607–619.

MILLERO, F.J., ZHANG, J.Z., FIOL, S., SOTOLONGO, S., ROY, R., LEE, K. & MANE, S. 1993. The use of buffers to measure the pH of seawater. *Marine Chemistry*, **44**, 143–152.

MORÁN, X.A.G. & ESTRADA, M. 2002. Phytoplanktonic DOC and POC production in the Bransfield and Gerlache Straits as derived from kinetic experiments of ^{14}C incorporation. *Deep-Sea Research II*, **49**, 769–786.

ROY, R.N., ROY, L.N., VOGEL, K.M., MOORE, C.P., PEARSON, T., GOOD, C.E., MILLERO, F.J. & CAMPBELL, D.M. 1993. Determination of the ionization constant of cabonic acid in seawater. *Marine Chemistry*, **44**, 249–268.

ROY, R.N., ROY, L.N., VOGEL, K.M., PORTER-MOORE, C., PEARSON, T., GOOD, C.E., MILLERO, F.J. & CAMPBELL, D.M. 1994. Erratum for: the dissociation constants of carbonic acid in seawater at salinities 5 to 45 and temperatures 0 to 45°C. *Marine Chemistry*, **45**, 337.

SCOTT, F.J., DAVIDSON, A.T. & MARCHANT, H.J. 2000. Seasonal variation in plankton, submicrometre particles and size-fractionated dissolved organic carbon in Antarctic coastal waters. *Polar Biology*, **23**, 635–643.

STAMMERJOHN, S.E., MARTINSON, D.G., SMITH, R.C. & IANNUZZI, R.A. 2008. Sea ice in the western Antarctic Peninsula region: spatio-temporal variability from ecological and climate change perspectives. *Deep-Sea Research II*, **55**, 2041–2058.

STOLL, M.H.C., DE BAAR, H.J.W., HOPPEMA, M. & FAHRBACH, E. 1999. New early winter f_{CO_2} data reveal continuous uptake of CO_2 by the Weddell Sea. *Tellus*, **B51**, 679–687.

TAKAHASHI, T., OLAFSSON, J., GODDARD, J.G., CHIPMAN, D.W. & SUTHERLAND, S.C. 1993. Seasonal-variation of CO_2 and nutrients in the high-latitude surface oceans - a comparative study. *Global Biogeochemical Cycles*, **7**, 843–878.

TAKAHASHI, T., SUTHERLAND, S.C., SWEENEY, C., POISSON, A., METZL, N., TILLBROOK, B., BATES, N., WANNINKHOF, R., FEELY, R.A., SABINE, C., OLAFSSON, J. & NOJIRI, Y. 2002. Global sea-air CO_2 flux based on climatological surface ocean pCO_2, and seasonal biological and temperature effects. *Deep-Sea Research II*, **49**, 1601–1622.

TAKAHASHI, T. *ET AL* 2009. Climatological mean and decadal change in surface ocean $pCO2$, and net sea-air CO_2 flux over the global oceans. *Deep-Sea Research II*, **56**, 554–577.

VAQUÉ, D., GUIXA-BOIXEREU, N., GASOL, J.M. & PEDRÓS-ALIÓ, C. 2002. Distribution of microbial biomass and importance of protists in regulating prokaryotic assemblages in three areas close to the Antarctic Peninsula in spring and summer 1995/96. *Deep-Sea Research II*, **49**, 847–867.

WANNINKHOF, R. 1992. Relationship between wind-speed and gas-exchange over the ocean. *Journal of Geophysical Research-Oceans*, **97**, 7373–7382.

WEISS, R.F. 1974. Carbon dioxide in water and seawater: the solubility of a non-ideal gas. *Marine Chemistry*, **2**, 203–205.

YAGER, P.L., WALLACE, D.W.R., JOHNSON, K.M., SMITH, W.O., MINNETT, P.J. & DEMING, J.W. 1995. The northeast water polynya as an atmospheric CO_2 sink - a seasonal rectification hypothesis. *Journal of Geophysical Research-Oceans*, **100**, 4389–4398.

ZAPATA, M., RODRIGUEZ, F. & GARRIDO, J.L. 2000. Separation of chlorophylls and carotenoids from marine phytoplankton: a new HPLC method using a reversed phase C-8 column and pyridine-containing mobile phases. *Marine Ecology Progress Series*, **195**, 29–45.